

RESEARCH ARTICLE

OPEN ACCESS

Theoretical And Numerical Slop Effect Study Of Non-Prismatic Beam On Fatigue Load And Location Failure Of Beam

Dr. Muhannad Al-Waily

University of Kufa / Faculty of Engineering / Mechanical Engineering Department, Iraq

ABSTRACT

In this paper, study of effect of slop of non-prismatic beam on the values of fatigue load required of failure the non-prismatic beam and the location of failure of beam. The study presented, theoretical study of non-prismatic beam with dynamic fatigue load in bending effect on the non-prismatic beam. And the compare of analytical results with numerical results presented and given good agreement with maximum error about 2.8% and minimum error about 1.3%.

The parameters study are the small to large diameter non-prismatic beam ratio, length to large diameter beam ratio, large diameter of beam, and the type of material using on the values of fatigue load, location of failure of beam, and fatigue stress applied to maximum fatigue stress of beam ratio and the location of maximum fatigue stress on non-prismatic beam. The length to large diameter ratio using from ' 10 to 100' and small to large diameter beam ratio using from ' 0 to 1 ' and the large beam diameters using are ' 5, 10, 20, 30, 40, 50, 75, 100, 150, 200, and, 250 mm'.

Keywords - Fatigue Study, Non-Prismatic Beam, Fatigue Location, Slope Beam Effect, Fatigue Effect.

I. INTRODUCTION

Most machinery and many structures do not operate under a constant load and stress. In fact, these loads and stresses are constantly changing. A good example of this is a rotating shaft such as the axle on a railroad car. The bending stresses change from tension to compression as the axle rotates. This constant change in stress can cause fatigue failure in which the material suddenly fractures. The process that leads to fatigue failure is the initiation and growth of cracks in the material. Fracture occurs when the crack grows so large that the remaining un-cracked material can no longer support the applied loads.

Beams that are deepened by haunches, to increase their moment resistance, and non-prismatic columns, such as those supporting crane girders in industrial buildings, are widely used in engineering practice. Members of variable stiffness are commonly used in many engineering structures, such as highway bridges, buildings, space and air-craft structures, as well as in many mechanical component and machines to achieve a better distribution of the internal stresses, reduce the dead load and sometimes to satisfy architectural and functional requirements. Since the members of variable cross section are involved in many important structures, it is necessary to analysis this kind of members with a greater precision, [5].

During the last years, light steel structures have been extensively used as being the most effective in practical application. The main advantages of such kind of structures are the effective usage of materials and quick erection as well as their good service characteristics. Over the past two decades, solution of

the buildings with tapered frames, manufactured from high-tensile steel, have become a standard. The use of automatic welding techniques minimizes the cost of such tapered members. Their contours are quite close to the bending moment diagram, so the bearing capacity of cross-sections is effectively utilized, [12].

Osman Asi [16], presented the failure analysis of a rear axle shaft used in an automobile which had been involved in an accident. The axle shaft was found to break into two pieces. The investigation was carried out in order to establish whether the failure was the cause or a consequence of the accident. An evaluation of the failed axle shaft was undertaken to assess its integrity that included a visual examination, photo documentation, chemical analysis, micro-hardness measurement, tensile testing, and metallographic examination.

S.K. Bhaumik et. Al. [17], A micro/hairline crack was noticed on a low speed, hollow shaft of a single stage helical gearbox during service. Though this had not resulted in a catastrophic failure, the shaft was withdrawn from service because of leakage of oil. Subsequent investigation revealed that the crack had initiated by fatigue at one of the keyway edges and progressed about 3/4 of the shaft periphery in a helical manner but had not given rise to final fracture of the shaft. The fatigue crack initiation was due to stress concentration arising from a depression mark at the keyway end surface. The problem was further aggravated due to inadequate radius at the keyway edges and rough machining marks. An analysis of the failure, together with recommendations for failure prevention, is presented in this paper.

Raman Bedi, Rakesh Chandra [18], In this investigation, rotating bending fatigue tests have been conducted on two types of unidirectional glass-fiber reinforced polymeric composites, having vinylester and Epoxy as matrix materials. It has been observed that the probabilistic distribution of fatigue-life of these glass-fiber reinforced composites, at a particular stress level, can be modeled by two-parameter Weibull distribution, with statistical co-relation coefficient values exceeding 0.90. Various methods have been used to obtain the parameters of Weibull distribution. Kolmogorov–Smirnov goodness-of-fit test has also been used to reinforce the above findings. The two-parameter Weibull distribution has also been employed to incorporate failure probability into S–N relationships.

In this research evaluated the values and location of fatigue load of non-prismatic beam with different large to small beam diameter, it's evaluated by analytical study and compare the results with numerical results evaluated by using of finite element method with using Ansys Ver. 14.

II. THEORETICAL STUDY

The stress study of cantilever beam subjected to the end bending fatigue load ' P ', as shown in Fig. 1, is,

$$\sigma_b = \frac{M.y}{I} = \frac{32.P.(l-x)}{\pi.D^3} \tag{1}$$

For prismatic beam, the maximum bending endurance stress at x=0 is,

$$\sigma_{b_{max}} = \sigma_e = \frac{32.P.l}{\pi.D^3} \tag{2}$$

From eq. 3. the maximum load can be subjecting are,

$$P_{failure} = \frac{\sigma_e.\pi.D^3}{32.l} \text{ (max. load)} \tag{3}$$

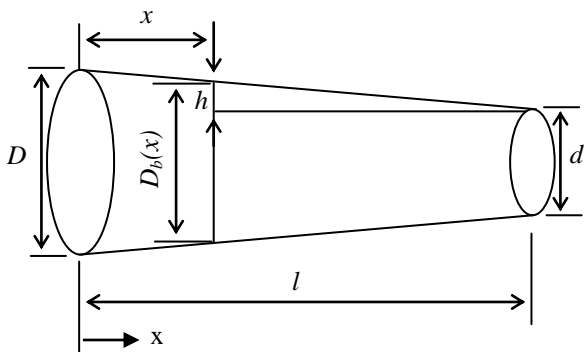


Fig. 1. Location of fatigue load subjected of beam.

For non-prismatic beam (see Fig. 2), the endurance stress is,

$$\sigma_e = \frac{32.P.(1-x)}{\pi.D_b^3(x)} \tag{4}$$

Where, Db(x) diameter of non-prismatic beam at any point of beam, can be defined as,

$$\frac{h}{(1-x)} = \frac{(D-d)}{2.l} \Rightarrow h = \frac{(D-d)}{2.l} . (1-x) \tag{5}$$

Then,

$$D_b(x) = d + 2.h = \left(d + \frac{(D-d)}{l} . (1-x) \right) \tag{6}$$

Then, by substitution Db(x), from eq. 6, into eq. 4, get,

$$\sigma_e = \frac{32.P.(1-x)}{\pi.\left(d + \frac{(D-d)}{l} . (1-x)\right)^3} \tag{7}$$

Then, can be rewrite eq. 7, as,

$$\left(d + \frac{(D-d)}{l} . (1-x) \right)^3 - \frac{32.P}{\pi.\sigma_e} . (1-x) = 0$$

$$\left(\frac{d}{D} + \left(1 - \frac{d}{D} \right) . \left(1 - \frac{x}{l} \right) \right)^3 = \frac{32.P.l}{\pi.\sigma_e.D^3} . \left(1 - \frac{x}{l} \right) \tag{8}$$

Eq. 8. get the relationship between the following variable,

1. The diameters ratio (d/D) and location failure of beam at maximum fatigue load subjected on the beam.
2. The required failure load at any point of beam for each diameter ratio (d/D). and,
3. The required failure load and diameter ratio (d/D) for each point of beam.

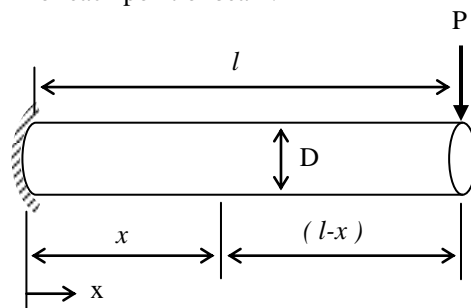
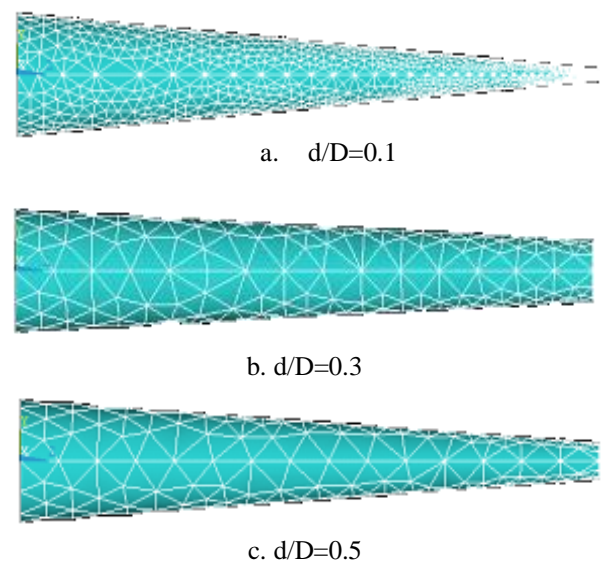


Fig. 2. Dimensions of Non-prismatic Beam.

III. NUMERICAL STUDY

In this method, the finite elements method was applied by using the ANSYS program(ver.14). The three dimensional model were built and the element (Solid Tet 10 node 187) were used. A sample of meshed beam for different large to small diameter is shown in Fig. 3.





d. $d/D=1$

Fig. 3. A sample of a meshed Non-Prismatic beam with different small to large diameter ratio.

IV. RESULTS AND DISCUSSION

The study of non-prismatic beam presented shown the effect of slop of beam on the fatigue load and location of failure of fatigue of non-prismatic beam. The dimensions of beam study are,

- Large diameters ' D ': 5, 10, 20, 30, 40, 50, 75, 100, 150, 200, 250 mm.
- Small to large diameters beam ratio ' d/D ': 0, 0.1, 0.2, 0.3, 0.4, 0.5, 0.6, 0.7, 0.8, 0.9, 1.
- Length to large diameter beam ratio ' L/D ': 10, 20, 30, 40, 50, 60, 70, 80, 90, 100.
- Material beam, [9],
 - Carbon Steel-1020 (endurance stress= $\sigma_e = 235$ Mpa)
 - Alloys Aluminum-3003 (endurance stress= $\sigma_e = 80$ Mpa)
 - Copper-CA110 (endurance stress= $\sigma_e = 100$ Mpa)

The Figs. 4 to 12. shown the compare between analytical and numerical results of required fatigue load of non-prismatic beam with different variable parameters of beam as large diameter, length to large diameter ratio and small to large diameter ratio for different beam material types. From the figures it can be seen that a good agreement between the analytical and numerical results, where, maximum error not expect 1.8%.

The figures below shown the results the effect of slop beam on the fatigue of non-prismatic beam as,

Figs. 13. to 15. Shown the required fatigue load at each point at the length of beam for different values of large diameter, length to large diameter ratio, and small to large diameters beam ratio, respectively. From the Fig. 13. shown the required fatigue load increasing with increasing large diameter of beam due to increasing of cross section area and moment of inertia of beam, and increasing at the end near the load supplied due to decreasing of distance of moment effect. And, form Fig. 14. Shown the required fatigue load decreasing with increasing of length to large diameter ratio due to increasing to length of beam and increasing the effect of moment. In addition to the fatigue load increasing with increasing of small diameter to large diameter ratio of beam due to increasing the area and moment of inertia effect of beam, and the required fatigue load decreasing at the end near the load supplied with decreasing the

diameters ratio due to decreasing of area and moment of inertia effect, as shown in Fig. 15.

Fig. 16. Shown the required fatigue load at each point at the length of beam for different materials beam, steel, copper, and aluminum beam. From figure shown the required fatigue load increasing with increasing of strength of beam.

Figs. 17. to 19. shown the effect of type of material on fatigue load of prismatic beam with various large diameter and length to large diameter ratio of beam, respectively. From figures shown that the fatigue load increasing with increasing of large diameter of beam due to increasing of cross section area and moment of inertia effect, and decreasing with increasing of length to large diameter ratio due to increasing of moment load effect.

Figs. 20. to 29. shown the effect of large diameter, small to large diameter ratio, length to large diameter, and the type of material on the fatigue load of non-prismatic beam. Form figures shown the fatigue load increasing with increasing the large diametric and small to large diameter of beam due to increasing of cross section effect of beam, and the fatigue load of beam decreasing with increasing of length to large diameter of beam due to increasing of length to beam and increasing of moment load effect, decreasing of large diameter of beam and decreasing of cross section area effect.

Figs. 30. to 33. shown stress distribution through length of beam with different of large diameter, small to large diameter ratio, length to large diameter ratio, and the type of material beam. Form figures shown that the fatigue stress not variable with variable of large diameters and length to large diameter ratio of beam. And the failure stress fatigue near the end to supplied load with decreasing of small to large diameter ratio of beam due to decreasing of cross section area effect near the end supplied of load.

Figs. 34. to 42. Shown the location of failure of beam due to fatigue load with different large diameter, small to large diameter ratio, length to large diameter ratio, and the types material of beam. From figures shown that the location of failure of beam not effect with variable of material type, large diameter of beam, and the length to large diameter of beam. And the location of failure of beam near to supported end of beam with increasing of small to large diameter ratio of beam to values of diametric ratio about 0.7, the location of failure at the supported location for diameter ratio form 0.7 to 1.

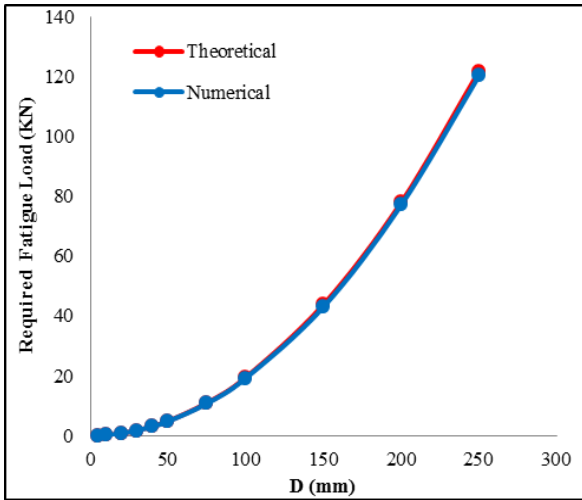


Fig. 4. Compare between Theoretical and Numerical Study of Fatigue load with different large diameter beam for small to large beam diameter ratio (0.5) and steel beam with, L/D=10.

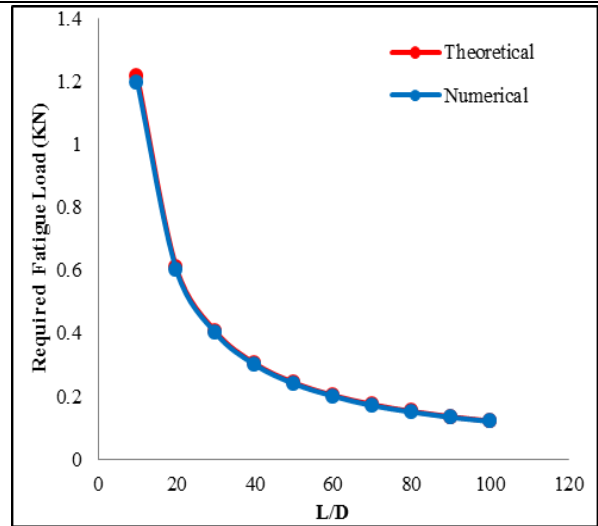


Fig. 7. Compare between Theoretical and Numerical Study of Fatigue load with different length to large diameter beam for small to large beam diameter ratio (0.5) and steel beam with, D=25 mm.

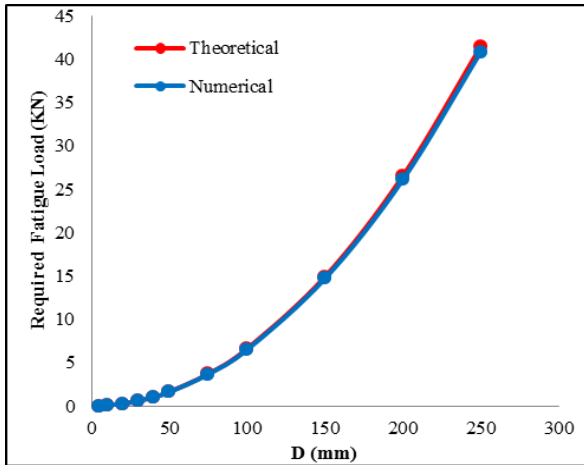


Fig. 5. Compare between Theoretical and Numerical Study of Fatigue load with different large diameter beam for small to large beam diameter ratio (0.5) and aluminum beam with, L/D=10.

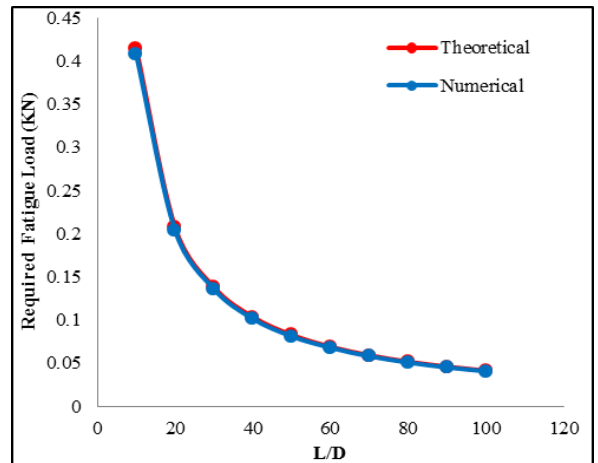


Fig. 8. Compare between Theoretical and Numerical Study of Fatigue load with different length to large diameter beam for small to large beam diameter ratio (0.5) and aluminum beam with, D=25 mm.

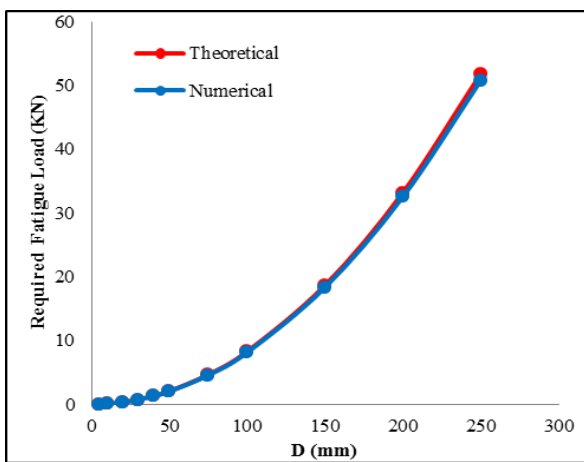


Fig. 6. Compare between Theoretical and Numerical Study of Fatigue load with different large diameter beam for small to large beam diameter ratio (0.5) and Copper beam with, L/D=10.

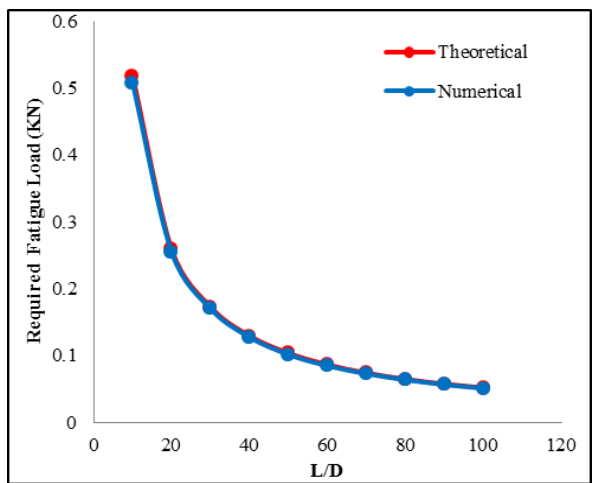


Fig. 9. Compare between Theoretical and Numerical Study of Fatigue load with different length to large diameter beam for small to large beam diameter ratio (0.5) and Copper beam with, D=25 mm.

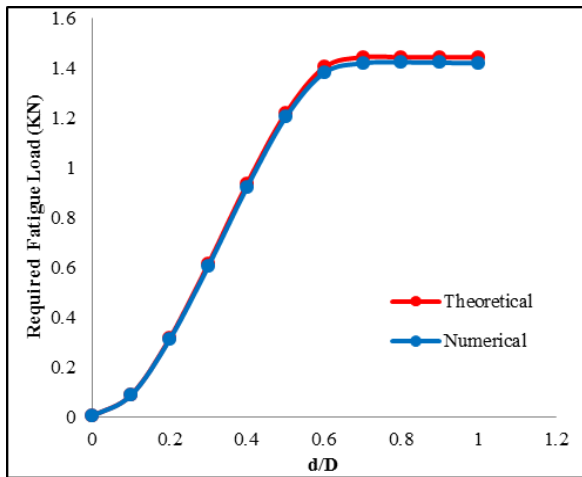


Fig. 10. Compare between Theoretical and Numerical Study of Fatigue load with different small to large diameter beam for length to large beam diameter ($L/D=10$) and steel beam with, $D=25$ mm.

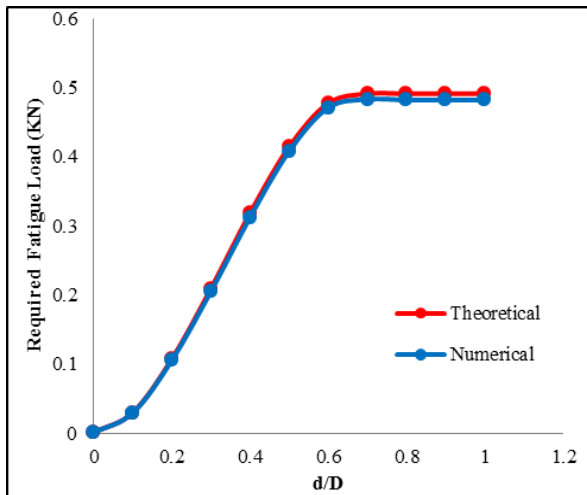


Fig. 11. Compare between Theoretical and Numerical Study of Fatigue load with different small to large diameter beam for length to large beam diameter ($L/D=10$) and aluminum beam with, $D=25$ mm.

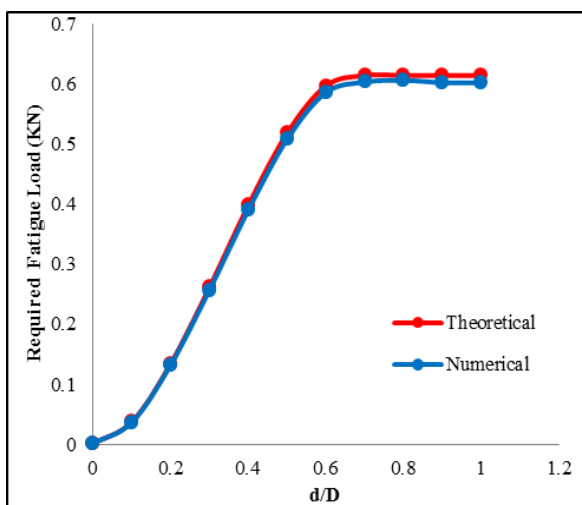


Fig. 12. Compare between Theoretical and Numerical Study of Fatigue load with different small to large diameter beam for length to large beam diameter ($L/D=10$) and Copper beam with, $D=25$ mm.

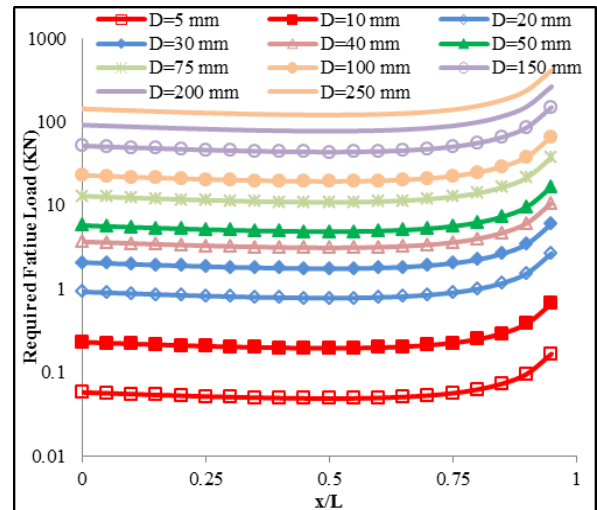


Fig. 13. Required of Fatigue load for each location of beam for steel for different large beam diameter for $d/D=0.5$, $L/D=10$.

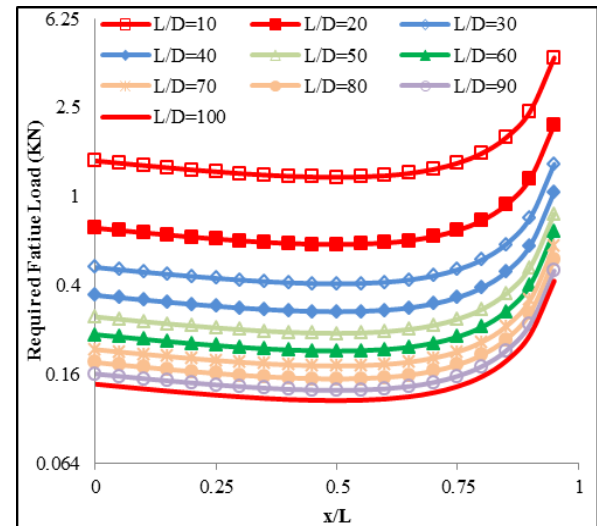


Fig. 14. Required of Fatigue load for each location of beam for steel, for different length to large diameter beam ratio for $d/D=0.5$, $D=25$ mm

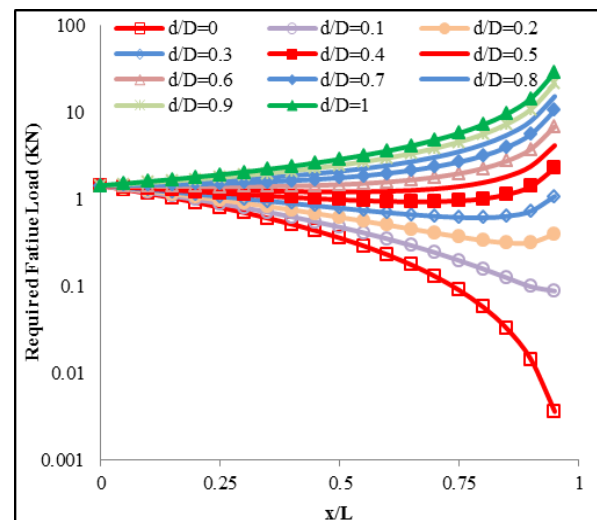


Fig. 15. Required of Fatigue load for each location of beam for steel, for different small to large beam diameter ratio for $L/D=10$, $D=25$ mm

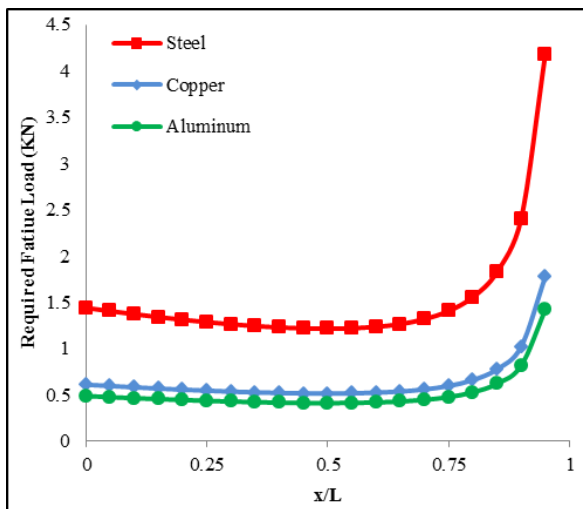


Fig. 16. Required of Fatigue load for each location of beam for different material, for $L/D=10$, $D=25$ mm , $d/D=0.5$.

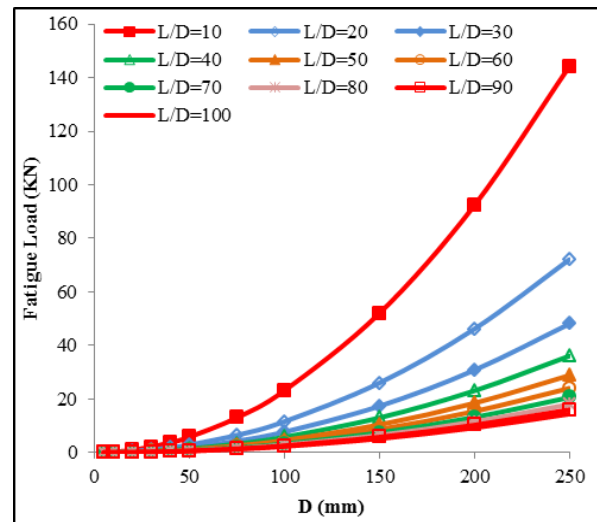


Fig. 19. Fatigue Load of Prismatic Beam with different large beam diameter with different length to diameter beam ratio for steel beam.

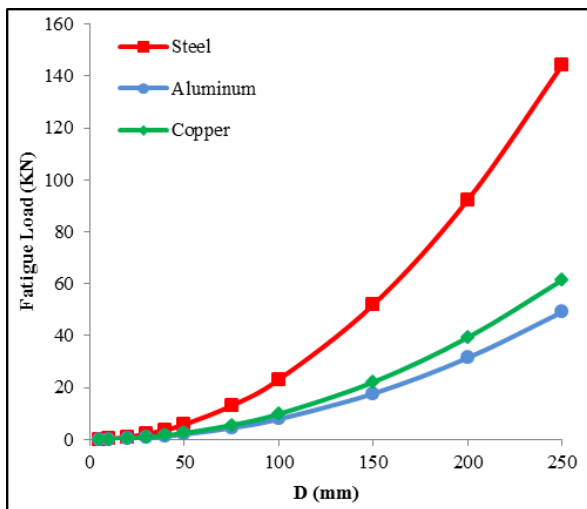


Fig. 17. Fatigue load for prismatic beam with different large diameter of beam for different material, for $L/D=10$

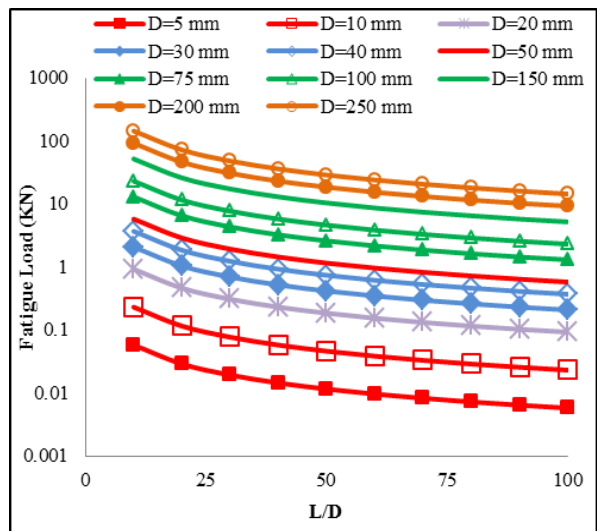


Fig. 20. Fatigue Load for Prismatic Beam with different length to diameter beam ratio with different large beam diameter for steel beam material.

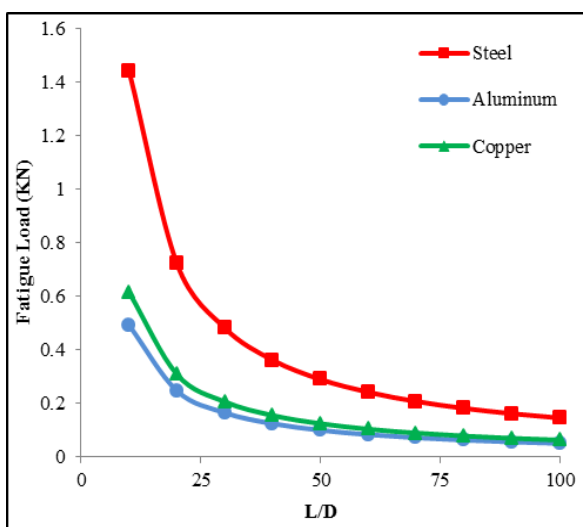


Fig. 18. Fatigue load for prismatic beam with different large diameter of beam for different material, for $D=25$ mm

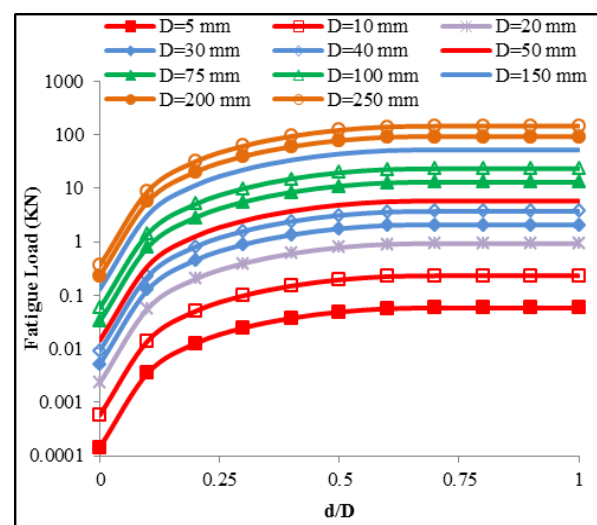


Fig. 21. Fatigue load with different small to large diameter beam ratio with different large beam diameter for steel beam with $L/D=10$.

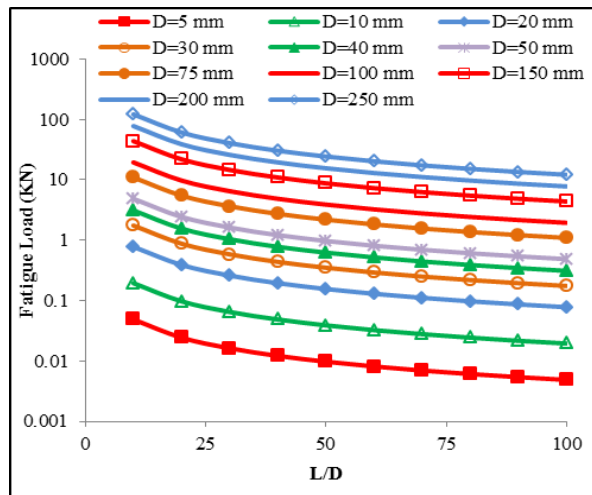


Fig. 22. Fatigue load with different length to large diameter beam ratio with different large beam diameter for steel beam with, $d/D=0.5$

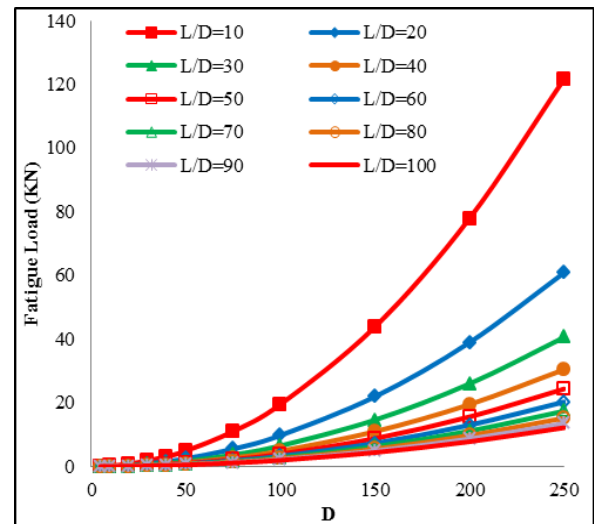


Fig. 25. Fatigue load with different large diameter beam with different length to large beam diameter ratio for steel beam with, $d/D=0.5$

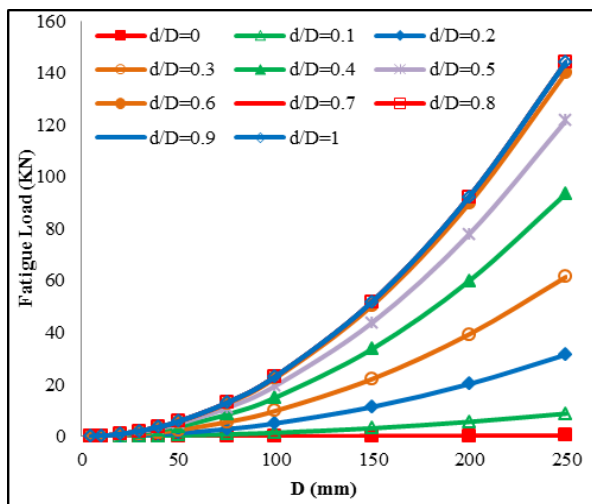


Fig. 23. Fatigue load with different large diameter beam with different small to large beam diameter ratio for steel beam with, $L/D=10$

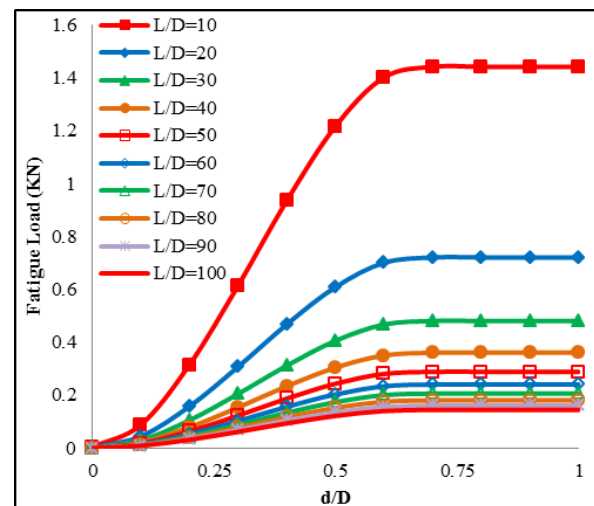


Fig. 26. Fatigue load with different small to large diameter beam ratio with different length to large beam diameter ratio for steel beam with, $D=25$ mm.

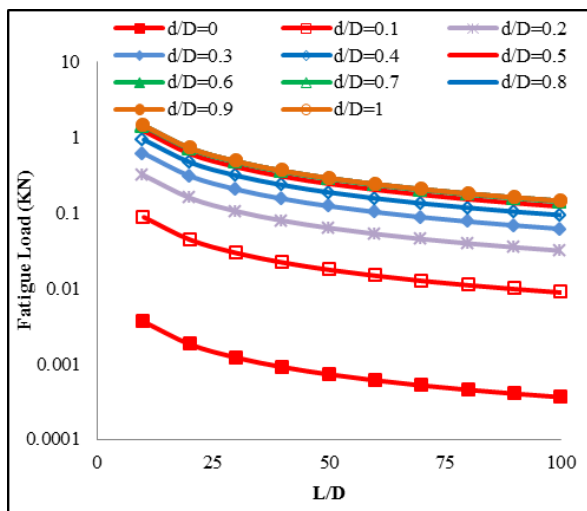


Fig. 24. Fatigue load with different length to large diameter beam ratio with different small to large beam diameter ratio for steel beam with, $D=25$ mm.

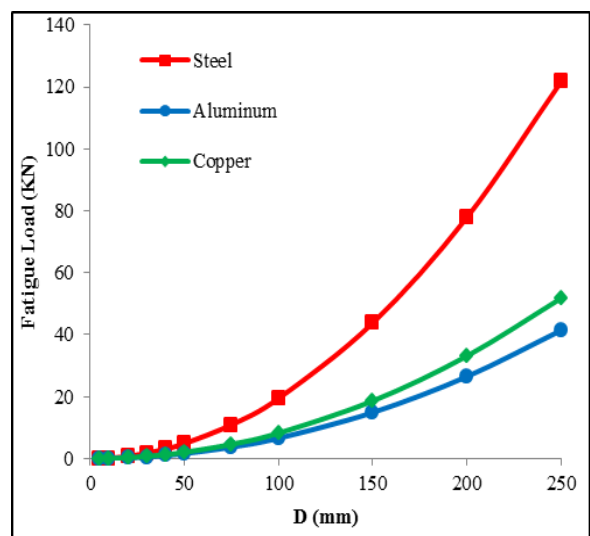


Fig. 27. Fatigue load with different large diameter beam with different materials beam with, $L/D=10$, $d/D=0.5$

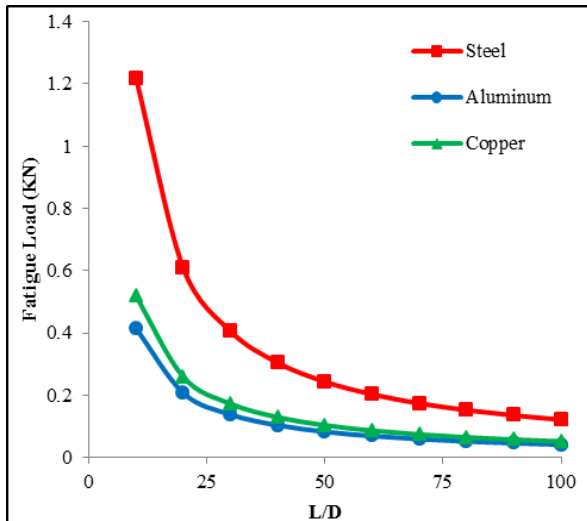


Fig. 28. Fatigue load with different length to large diameter beam ratio with different materials beam with, $D=25$ mm , $d/D=0.5$

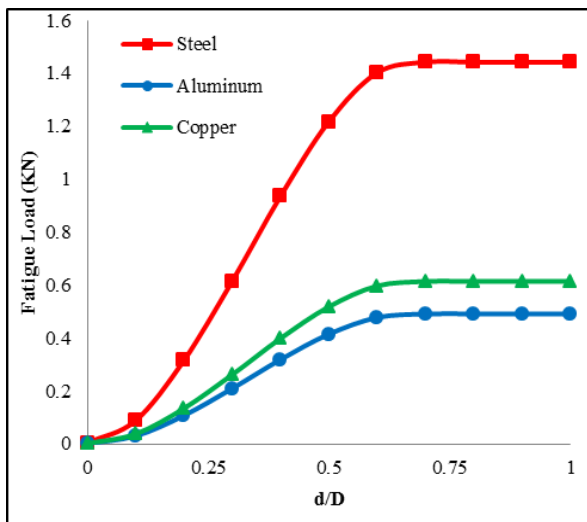


Fig. 29. Fatigue load with different small to large diameter beam ratio with different materials beam with, $L/D=10$, $D=25$ mm

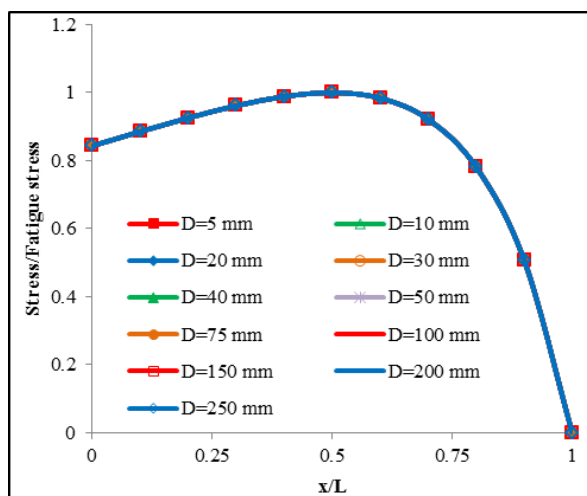


Fig. 30. Stress distribution through length of beam with different large beam diameter for steel beam with, $L/D=10$, $d/D=0.5$

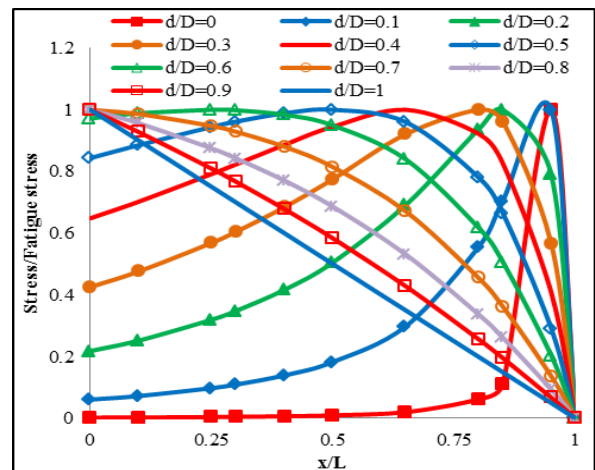


Fig. 31. Stress distribution through length of beam with different small to large beam diameter for steel beam with, $L/D=10$, $D=25$ mm.

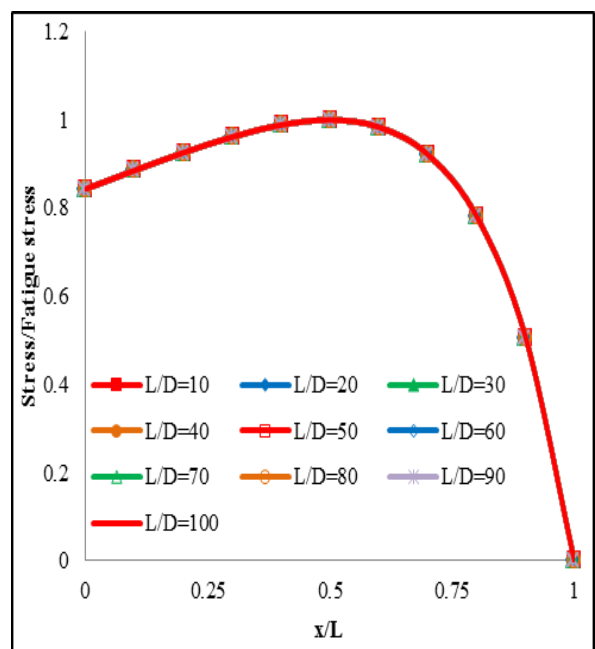


Fig. 32. Stress distribution through length of beam with different length to large diameter beam ratio for steel beam with, $d/D=0.5$, $D=25$ mm.

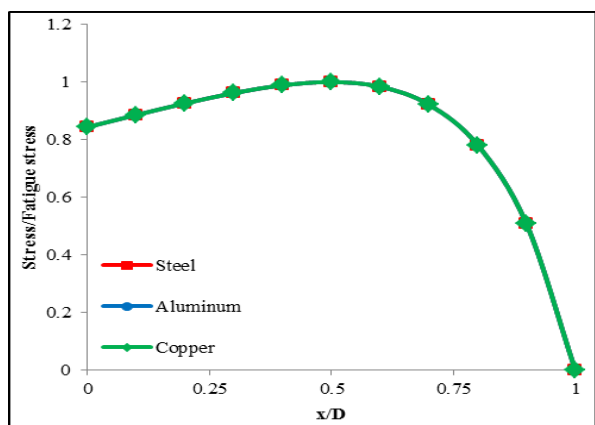


Fig. 33. Stress distribution through length of beam for different materials beam with, $L/D=10$, $d/D=0.5$, $D=25$ mm

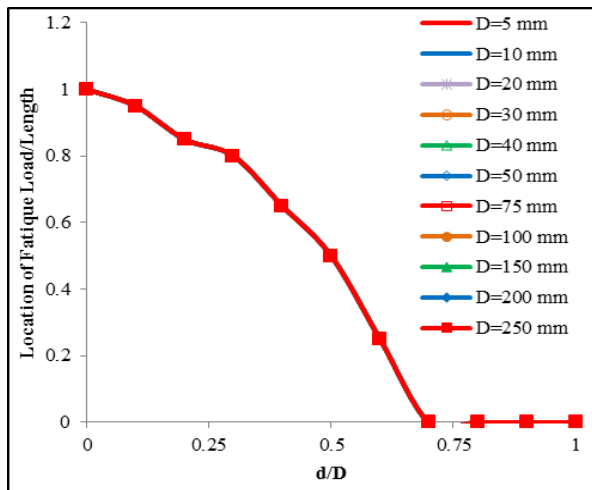


Fig. 34. Location failure of beam with different small to large diameter ratio of beam for various large diameter beam for steel beam with $L/D=10$

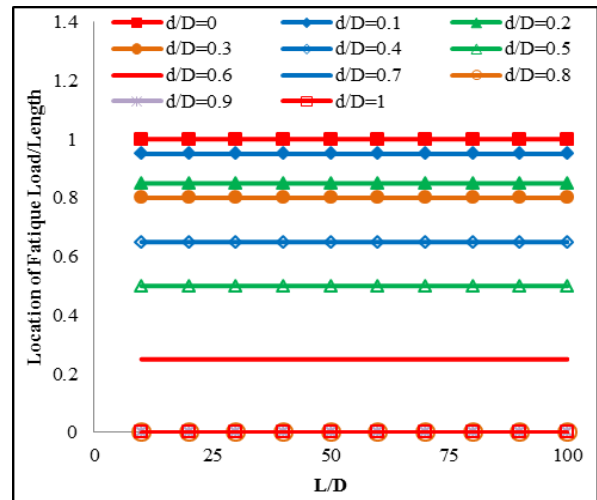


Fig. 37. Location of failure of beam with different length to large beam diameter ratio for various small to large beam diameter ratio for steel beam with, $D=25$ mm.

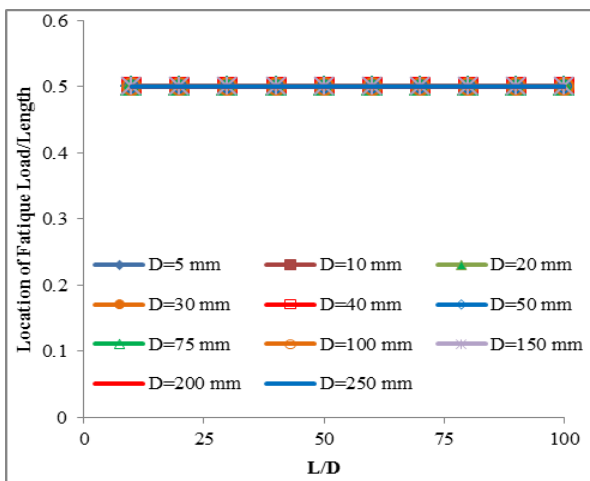


Fig. 35. Location of failure of beam with different length to large diameter beam ratio for various large diameter of steel beam with, $d/D=0.5$

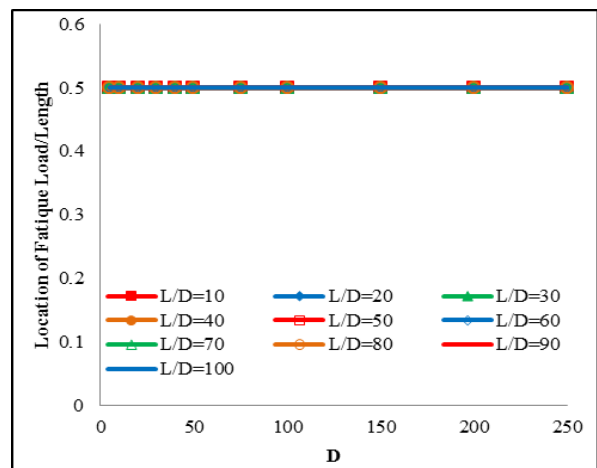


Fig. 38. Location of failure of beam with different large diameter of beam for various length to large diameter ratio for steel beam with, $d/D=0.5$

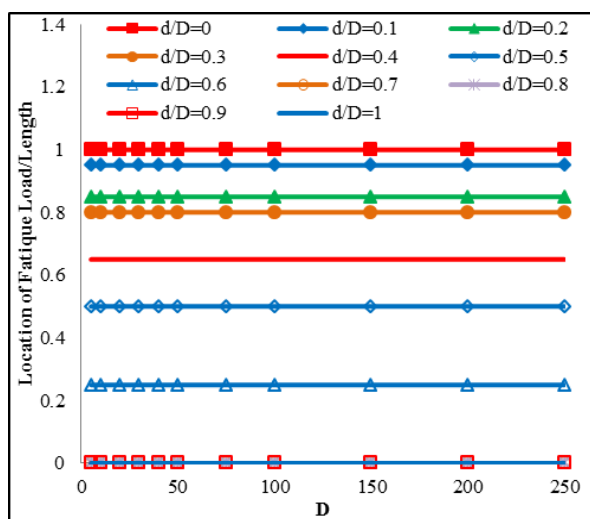


Fig. 36. Location of failure of beam with different large beam diameter for various small to large beam diameter ratio for steel beam with, $L/D=10$

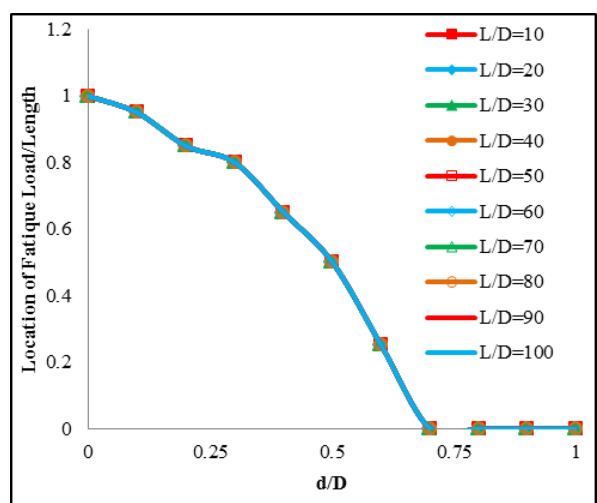


Fig. 39. Location of failure of beam with different small to large diameter ratio for various length to large diameter ratio for steel beam with, $D=25$ mm

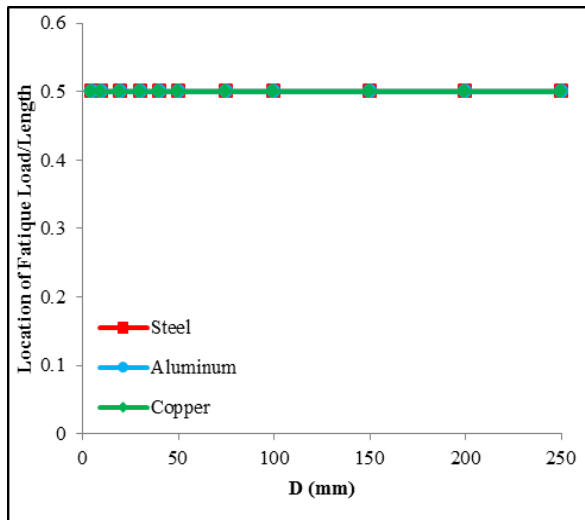


Fig. 40. Location of failure of beam with different large diameter beam for various materials beam with, L/D=10, d/D=0.5

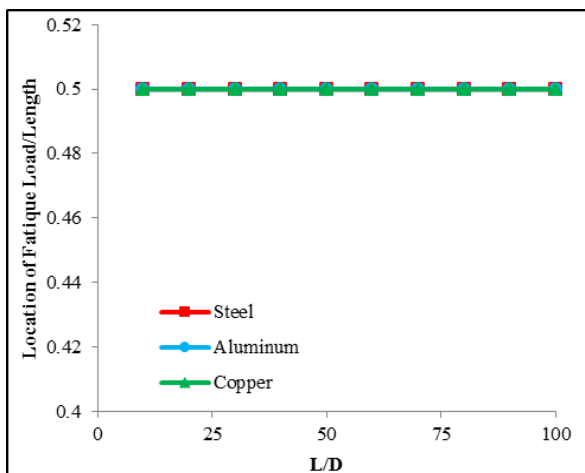


Fig. 41. Location of failure of beam with different large diameter beam for various materials beam with, D=25 mm, d/D=0.5

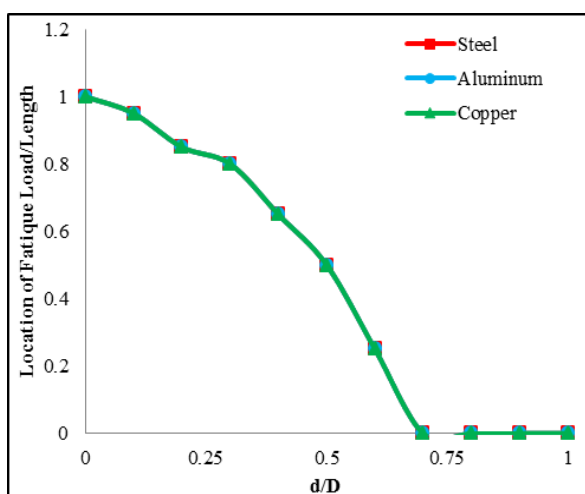


Fig. 42. Location of failure of beam with different small to large diameter ratio for various material of beam with, L/D=10, D=25 mm

V. CONCLUSION

From results presented shown the main conclusion of effect of slop of non-prismatic beam on the fatigue load as,

1. A comparison made between analytical results from solution of analysis equation of non-prismatic beam with beam slop effect with numerical results by finite elements method shows a good approximation.
2. The fatigue load increasing with increasing of area of beam and decreasing with increasing the length of beam. And, the fatigue load decreasing with decreasing small to large diameter ratio of beam. In addition to, the fatigue load increasing with increasing of strength of material of beam.
3. The location failure of beam near the supported end of beam with increasing of small to large diameter ratio of beam. And, the location of failure of beam not effect with variable of large diameter, length to large diameter ratio of beam, strength of material of beam.
4. The fatigue load and location of failure of beam not effect with different small to large diameter ratio of beam form 0.7 to 1.

REFERENCES

- [1] H. J. Al_Gahtani and M. S. Khan 'Exact Analysis of Non-prismatic Beams' Journal of Engineering Mechanics/ November 1998.
- [2] John W. Fisher, Karl H. Frank, Manfred A. Hirt, and Bernard M. McNamee 'Effect of Weldments on the Fatigue Strength of Steel Beams' Fritz Engineering Laboratory Report No. 334.2, 1969.
- [3] Kiang Hwee Tan 'design of Non-Prismatic RC Beams Using Strut-and-Tie Models' Journal of Advance Concrete Technology, Vol. 2, No. 2, 249-256, June 2004.
- [4] Mumuni I. 'A Finite Element Model for the Analysis and Optimal Design of Beams and Plates with Variable Flexural Rigidity' Thesis Presented to Vanderbilt university at Nashville, Tenn in Partial Fulfillment of the requirement, for the Degree of Doctor of Philosophy, 1983.
- [5] M. S. Khan and H. J. Al_Gahtani 'Analysis of Continuous Non-Prismatic Beams Using Boundary Procedures' The Fourth Saudi Engineering Conference, Vol. 2, No. 5, 1995.
- [6] Nasereddin El_Mezaini, Can Baikaya and Ergin 'Analysis of Frames with Non-Prismatic Members' Journal Structural Division ASCE, Vol. 117, No. 6, 1573-1592, 1991.
- [7] P. RUTA 'Dynamic Stability Problem of a Non-Prismatic Rod' Journal of Sound and Vibration, Vol. 250, No. 3, 445-464, 2002.

- [8] Resend J. W. and Doyle B. J. '*Non-Prismatic and Effective Non-Prismatic Three Dimensional Beam Finite Element*' Computer and Structures, Vol. 41, No.1, 71-77, 1981.
- [9] Robert L. Norton "*Machine Design*" Pearson Education, Inc., 2006.
- [10] Sen Yung Lee, Huei Yaw Ke and Yee Hsiung Kuo '*Exact Static Deflection of a Non-Uniform Bernoulli-Euler Beam with General Elastic Restraints*' Comput. & Struct., Vol. 36, No. 1, 91-97, 1990.
- [11] S. Z. Al-Sadder and H. Y. Qasrawi '*Exact Secant Stiffness Matrix For Non-Prismatic Beam-Columns With Elastic Semirigid Joint Connections*' Emirates Journal for Engineering Research, Vol. 9, No. 2, 127-135, 2004.
- [12] Vaidotas Sapalas, Michail Samofalov, Viaceslavas Sarakinas '*FEM Stability Analysis of Tapered Beam-Columns*' Journal of Engineering and Management, Vol. 11, No. 3, 211-216, 2005.
- [13] Marc J. A. Braem, Paul Lambrechts, Sonia Gladys and Guido Vanherle "*In-vitro fatigue behavior of restorative*" Volume 11 , Issue 2 , March 1995, PP 137-141.
- [14] Ali S. Hammood, Muhannad Al-Waily, and Ali Abd. Kamaz '*Effect of Fiber Orientation on Fatigue of Glass Fiber Reinforcement Epoxy Composite Material*' The Iraqi Journal For Mechanical And Material Engineering, Vol. 11, No. 2, 2011.
- [15] Y Y. Al-Assaf and H. El Kadi "*Fatigue life prediction of unidirectional glass fiber/epoxy composite laminae using neural networks*" Volume 53, Issue 1, July 2001, PP. 65-71.
- [16] Osman Asi '*Fatigue failure of a rear axle shaft of an automobile*' Engineering Failure Analysis, Vol. 13, pp. 1293-1302, 2006.
- [17] S.K. Bhaumik, R. Rangaraju, M.A. Parameswara, M.A. Venkataswamy, T.A. Bhaskaran, R.V. Krishnan '*Fatigue failure of a hollow power transmission shaft*' Engineering Failure Analysis, Vol. 9, pp. 457-467, 2002.
- [18] Raman Bedi, Rakesh Chandra '*Fatigue-life distributions and failure probability for glass-fiber reinforced polymeric composites*' Composites Science and Technology, Vol. 69, pp. 1381-1387, 2009.